Journal of Sound and Vibration (2002) **257**(1), 3–18
doi:10.1006/jsvi.2001.4162, available online at http://www.idealibrary.com on IDEAL®

DYNAMIC ANALYSIS OF AN AUTOMATIC WASHING MACHINE WITH A HYDRAULIC BALANCER

S. Bae, J. M. Lee, Y. J. Kang, J. S. Kang† and J. R. Yun‡

School of Mechanical and Aerospace Engineering, Seoul National University, San 56-1 *Shinlim-dong, Kwanak-gu, Seoul* 151-742, *South Korea. E-mail: yeonjune@snu.ac.kr*

(*Received* 27 *February* 2001, *and in final form* 4 *January* 2002)

A mathematical model of a hydraulic balancer in steady state condition was derived from a whirling model of a vertical axis washing machine, with the aim of implementing a dynamic analysis of an automatic washing machine during spin drying mode. The centrifugal force acting on the hydraulic balancer depends on the centroidal distance of the fluid in the hydraulic balancer, and the centroidal distance is a function of an eccentricity of the geometric center of the hydraulic balancer from the axis of rotation. A mathematical model of the hydraulic balancer in steady state is validated by the experimental result of the centrifugal force. Experiments were performed on a washing machine during spin drying mode, and results were compared with the simulation result. The parameters affecting the vibration of the washing machine were investigated by the parameter study.

1. INTRODUCTION

Besides basic functions such as washing and spin drying, low vibration characteristic is becoming an important performance index of washing machines. In an automatic washing machine, the drying process involves the spin motions of a basket, while the washing process involves the oscillating motions of the basket. The power is transmitted to the identical rotating axis of the basket through a belt from a motor during both the washing and spin drying. After the washing mode, the laundry is dried by the spin drying mode. During the washing mode, clothes tend to clump, creating an unbalance mass in the basket. That unbalance mass can cause serious vibration problems when the basket spins with relatively high speed during the drying cycle. The amount of the unbalance mass is dependent on both the weight of the laundry and the condition of the washing mode. Thus, it is difficult to estimate the unbalance mass accurately and to design the spring stiffness or damper coefficient of a suspension system for washing machines. In these cases, it will be more appropriate to use a variable dynamic balancer for the purpose of reducing the excessive vibration of washing machines.

One type of dynamic balancer that can be used of washing machines is a hydraulic balancer, which contains salt water and is attached at the upper rim of the basket. There are several kinds of fluid that may be used in the hydraulic balancer: fresh water, salt water, oil and liquid mercury. However, liquid mercury is dangerous for human when the leakage takes place, even though it may be the best to be used. Moreover, oil may contaminate the

†Now at: Daewoo Motor Co. Ltd., Chongchon-dong 199, Bupyong-gu, Inchon 403–714, South Korea.
‡Now at: Hyundai Motor Co. Ltd., Jangduk-ri 772-1, Namyang-myun Hwasung-gun, Kyunggi-do 445-850, South Korea.

0022-460X/02/$35.00

laundry. Why salt water is used as the working fluid in the hydraulic balancer will be discussed. The hydraulic balancer, rotating together with the basket and acting as a counter mass, locates the salt water to the opposite side of the unbalance, due to the inherent nature of fluids. Therefore, such a feature makes the hydraulic balancer more effective than a solid balancer. The amount and distribution of the fluid counter mass are determined by the rotating speed and the internal structure of the balancer.

Washing machines may be categorized as a horizontal axis washer and a vertical axis washer. Depending on their motion and suspension location, vertical axis washers are further divided into two types: agitator-type and pulsator-type. In the former type the washing unit is mounted on springs, while in the latter type the washing unit is suspended from four suspension rods. Horizontal axis or drum-type washers are manufactured in Europe, agitator-type washers in the United States, and pulsator-type washers in Asia. In order to analyze the vibration of washers, different models are needed for these different types.

Bagepalli [1] investigated the dynamic modelling of agitator-type washers. He studied two concepts for suspension systems: non-translating fixed node design (NTFN) and translating free node design (TFN). He concluded that the NTFN concept is useful for minimizing the walking force, whereas the TFN concept, which was found to be the preferred design, is useful for minimizing transient excursions. Turkay *et al.* [2, 3] presented a dynamic model for horizontal axis washers. They carried out theoretical and experimental dynamic analyses for transient and steady state conditions. Later, the validated model was used to optimize the spring stiffness of suspension and the two dry-friction coefficients of shock absorber and lateral damper [4, 5]. They used an optimization routine that minimizes the maximum displacements for transient and steady state conditions subjected to the constraint of inequality of stepping forces. Recently, Conrad and Soedel [6] discussed extensively the qualitatively observed characteristics and mechanism of walk by using simplified models for both horizontal and vertical axis washers. Based on numerical simulations, they concluded that the vertical axis washing machine tends to walk in bounded region while the horizontal axis washing machine tends to walk unbounded in a direction dictated by the rotational direction of the wash basket.

Although there have been a number of studies on the dynamic analysis of vertical and horizontal axis washing machines, the analysis of pulsator-type washers with a hydraulic balancer has not yet been reported. In most of actual pulsator-type washing machine, the hydraulic balancer is used to reduce the vibration caused by the unbalance mass of the laundry. In this paper, in order to investigate how the hydraulic balancer affects the washing machine, a mathematical model of the hydraulic balancer for steady state condition is formulated and validated by experimental results. The mathematical model of the hydraulic balancer is then combined into a dynamic model of the vertical axis washing machine. Numerical simulations are compared with measurements for the radial accelerations of the tub during spin drying. The parameters affecting the vibration of the washing machine are also investigated.

2. MATHEMATICAL MODEL

A vertical axis washing machine of pulsator-type, as schematically illustrated in Figure 1, is considered in this study. The tub, which is a non-rotating part and to which the motor-driving axis assembly is attached at the bottom surface, is suspended by four rods comprising a spring–damper system. The torque is transmitted through the driving axis to the basket which is contained within the tub. A hydraulic balancer as shown in Figure 2 is

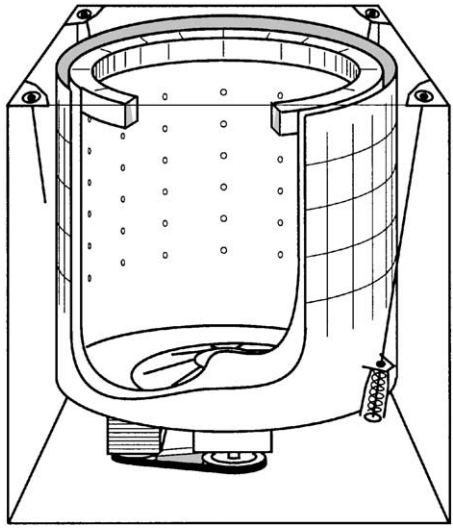

Figure 1. Illustration of a vertical axis washing machine.

Figure 2. The hydraulic balancer.

made of a plastic tube filled with salt water and is fixed at the upper part of the basket. Thus, the hydraulic balancer rotates together with the basket and the laundry. During spin drying, the hydraulic balancer plays an important role in reducing the centrifugal force generated by the unbalance mass of the basket and the laundry. Such a reduction can be effective when the hydraulic balancer moves the internal salt water in the opposite direction to the unbalance mass. This physical phenomenon can be explained by using a whirling model [7] as shown in Figure 3(a), which is the top view of an equivalent two-degree-of-freedom model of a washing machine in an arbitrary position. When the mass center, C, of the rotating unit having total mass, m, and eccentricity, e, from the geometric center, S, does not coincide with the center of rotation, O, the rotation of the basket produces a centrifugal force that can cause excessive motions. In steady state, if the rotational frequency ω is much higher than the natural frequency ω_n, the mass center tends to coincide with the center of rotation and the amplitude of the motion becomes almost equal to the initial eccentricity e, as shown in Figure 3(b). In the mean time, as a result of the centrifugal force, the fluid in the tube will move outward from the center of rotation in the opposite direction of the unbalance mass, thus decreasing the total eccentricity e. In general, the rotating frequency of the pulsator-type washing machine is high enough to be governed by the above condition.

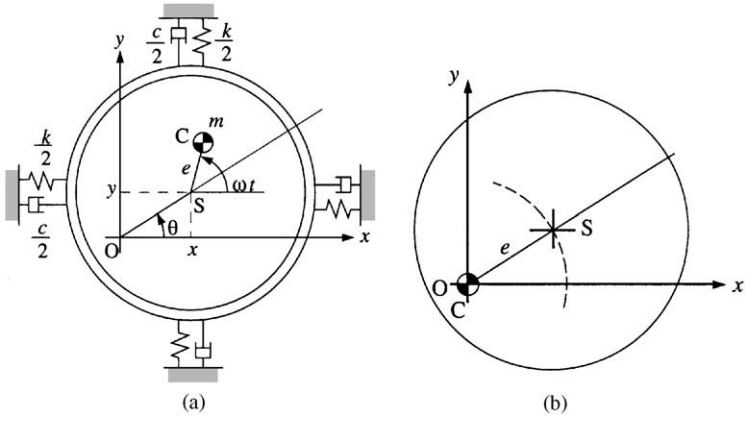

Figure 3. A whirling model of the washing machine: (a) a top view, and (b) steady state behavior when $\omega \gg \omega_n$.

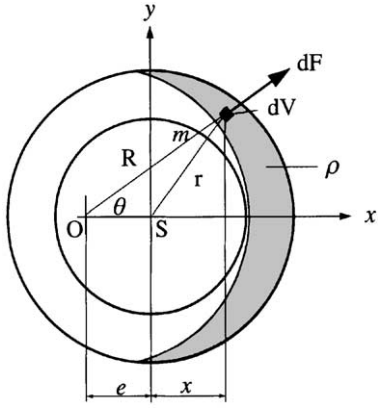

Figure 4. Centrifugal force of the hydraulic balancer.

Although the hydraulic balancer is very effective in reducing the centrifugal force of the unbalance mass in steady state, it may increase the unbalance in transient state. To prevent those unfavorable motions that may be caused by the hydraulic balancer, provisions such as orifices and obstructions are made inside the tube. In this paper, the analysis is limited to the steady state condition due to complexity of the transient behaviour of hydraulic balancers.

2.1. MATHEMATICAL MODEL OF A HYDRAULIC BALANCER

Figure 4 shows a horizontal cross-section of a hydraulic balancer. The centrifugal force $\mathrm{d}F$ acting on the incremental volume $\mathrm{d}V$ of the fluid within the hydraulic balancer can be written as

$$\mathrm{d}F = \rho R \omega^2 \, \mathrm{d}V, \tag{1}$$

where ρ represents the density of the fluid, R the distance from the axis of rotation, and ω the rotation speed. By assuming that the density of the fluid is uniform and the rotation

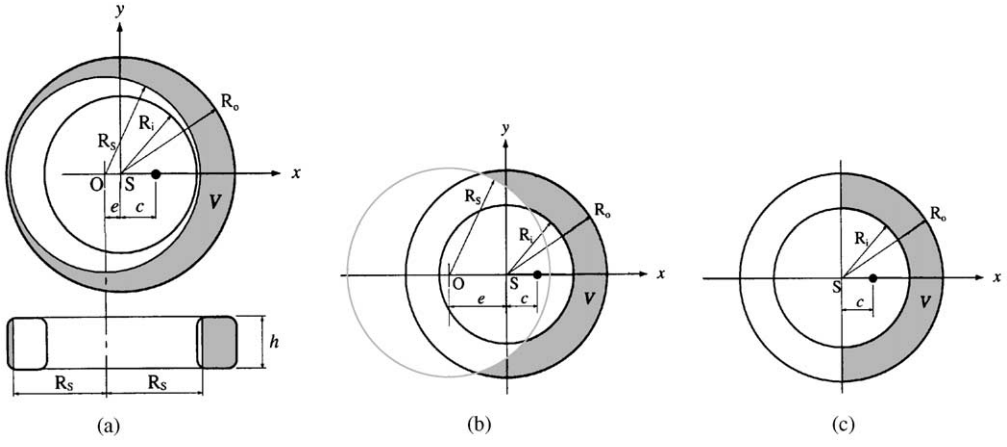

Figure 5. Centroid of the fluid in the hydraulic balancer: (a) when $e < \bar{e}$, (b) when $e > \bar{e}$, and (c) when $e \gg \bar{e}$.

speed is kept constant, the total centrifugal force F acting on the centroid of the fluid is given as

$$F = \int \mathrm{d}F \cos\theta = \rho\omega^2 e \int \mathrm{d}V + \rho\omega^2 \int x \, \mathrm{d}V. \tag{2}$$

By letting c be the distance of the centroid of fluid from the center of the basket in the x-direction and taking $c = \int x \, \mathrm{d}V / \int \mathrm{d}V$, we can rewrite equation (2) as

$$F = m\omega^2(e + c), \tag{3}$$

where m represents the total mass of the fluid. Equation (3) shows that the centrifugal force depends not only on the eccentricity e of the unbalance mass but also on the centroidal distance c of the fluid. It is now necessary to calculate the centroidal distance c of the tube.

When the eccentricity is small, the fluid within the tube in the steady state condition is shown in Figure 5(a). The centrifugal force acting on the fluid is so large that the inner surface of the fluid may be assumed to be almost vertically flat. It is also assumed that the cross-section of the hydraulic balancer is rectangular and the orifice effect of the tube is negligible in the steady state. If the volumetric ratio of the fluid to the tube is q, the total volume of the fluid is

$$V = q\pi(R_o^2 - R_i^2)\, h = \pi(R_o^2 - R_s^2)\, h, \tag{4}$$

where R_i and R_o are the inner and outer radii of the tube, respectively, and R_s is the radius of the inner surface of the fluid from the rotating axis. Thus, from equation (4), we can obtain

$$R_s = \sqrt{(1 - q)R_o^2 + qR_i^2}. \tag{5}$$

By definition centroidal distance can be calculated as

$$c = \frac{\int x \, \mathrm{d}V}{\int \mathrm{d}V}, \tag{6}$$

where $\int \mathrm{d}V$ is the total volume $V = \pi(R_0^2 - R_s^2)h$, and $\int x \mathrm{d}V$ can be calculated from Figure 5(a) as

$$\int x \mathrm{d}V = 2h\left(\int_{-R_o}^{R_o} x\sqrt{R_0^2 - x^2}\mathrm{d}x - \int_{-R_s-e}^{R_s-e} x\sqrt{R_s^2 - (x+e)^2}\,\mathrm{d}x \right) = \pi R_s^2 eh. \tag{7}$$

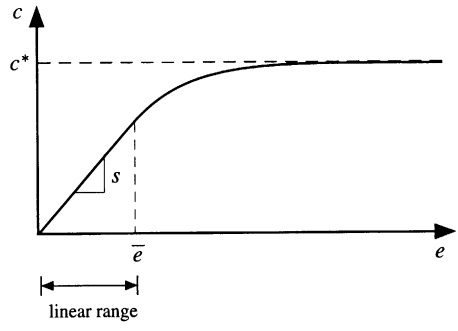

Figure 6. Centroid change due to eccentricity.

Therefore, the centroidal distance may be written as

$$c = \frac{R_s^2 e}{R_0^2 - R_s^2} \equiv se, \tag{8}$$

where $s \equiv R_s^2/(R_0^2 - R_s^2)$. Note that equation (8) is valid only when $e \leqslant \bar{e} = R_s - R_i$. Hence, when the eccentricity is small, it may be found from equation (8) that the centroid of the fluid is linearly proportional to the eccentricity and that the coefficient s depends on the inner and outer radii of the tube and the volumetric ratio of the fluid to the tube.

When the eccentricity is relatively large, i.e., $e > \bar{e}$, the fluid within the tube may be placed as shown in Figure 5(b). Since washing machines generally operate in the range of $e \leqslant \bar{e}$, the limit case to be used for efficient computations is as shown in Figure 5(c). In this case, the fluid in the tube moves to one side and acts like a rigid counter mass. The limit value of the centroid, c^*, can be calculated by simple integration:

$$c^* = \frac{2h\int_0^{q\pi}\int_{R_i}^{R_o} r^2 \cos\theta \mathrm{d}r\mathrm{d}\theta}{2h\int_0^{q\pi}\int_{R_i}^{R_o} r\mathrm{d}r\mathrm{d}\theta} = \frac{2}{3}\frac{R_o^2 + R_o R_i + R_i^2}{R_o + R_i}\frac{\sin(q\pi)}{q\pi} \tag{9}$$

and the centroid becomes a constant as the eccentricity grows extremely large. Thus, the centroid of the fluid is summarized as follows:

$$c = \begin{cases} se, & e < \bar{e}, \\ c^*, & e \to \infty\,. \end{cases} \tag{10}$$

Equation (10) represents the relation between the centroid and the eccentricity for two cases: small and very large eccentricities. For immediate case, it is difficult to obtain exact relationship between the centroid and the eccentricity. Therefore, for the purpose of numerical simulations, two equations in equation (10) should be connected by two conditions: C^1-continuity at $e = \bar{e}$ and c^* as $e \to \infty$, as shown in Figure 6. Using arctan function, equation (10) may now be defined as

$$c = \begin{cases} se & e < \bar{e}, \\ a_1 + a_2 \arctan\{a_3(e - \bar{e})\} & e \geqslant \bar{e}. \end{cases} \tag{11}$$

The coefficients in second equation can be found by applying the conditions, resulting $a_1 = s\bar{e}$, $a_2 = \frac{2}{\pi}(c^* - a_1)$ and $a_3 = s/a_2$. Thus, equation (10) can be re-written as

$$c = \begin{cases} se, & \\ s\bar{e} + \dfrac{2}{\pi}(c^* - s\bar{e}) \quad \arctan\left(\dfrac{\pi(e - \bar{e})}{2(c^* - s\bar{e})}\right), & e < \bar{e} \\ & e \geqslant \bar{e}. \end{cases} \tag{12}$$

For the washing machine considered in this study, the characteristic values of the hydraulic balancer, $\bar{e} = 28{\cdot}6$ mm, $s = 4{\cdot}373$ and $c^* = 150{\cdot}0$ mm were obtained when $q = 0{\cdot}5$, and $R_i = 206$ mm, $R_o = 260$ mm, and its schematic plot is shown in Figure 6.

2.2. DYNAMIC MODEL FOR A VERTICAL AXIS WASHING MACHINE

Figure 7 shows a dynamic model for the vertical axis washing machine considered in this paper. In Figure 7, the $X_1X_2X_3$ co-ordinates represent a global reference frame, and the body-fixed $x_1x_2x_3$ co-ordinates embedded in the tub represent a rotating frame whose origin is located at the mass center of the basket. The vectors **s** and **r** are the position vectors with respect to the global reference frame and the rotating frame respectively. The vectors **x** and $\boldsymbol{\phi}$ are, respectively, the translational and rotational displacement vectors with respect to the global reference frame. The superscripts $(\cdot)^b$, $(\cdot)^t$, $(\cdot)^u$, $(\cdot)^h$, $(\cdot)^{S_i}$, and $(\cdot)^{C_i}$, respectively, denote the basket, the tub, the unbalance mass, the hydraulic balancer, the ith connecting point of the rod to the tub, and the ith connecting point of the rod to the case. For example, $\mathbf{x}^b = [x_1^b \;\; x_2^b \;\; x_3^b]^{\mathrm{T}}$ and $\boldsymbol{\phi} = [\phi_1 \;\; \phi_2 \;\; \phi_3]^{\mathrm{T}}$ represent the translational and rotational displacement vectors of the basket. Thus, the dynamic behavior of the washing system is described with these six components of displacement vectors.

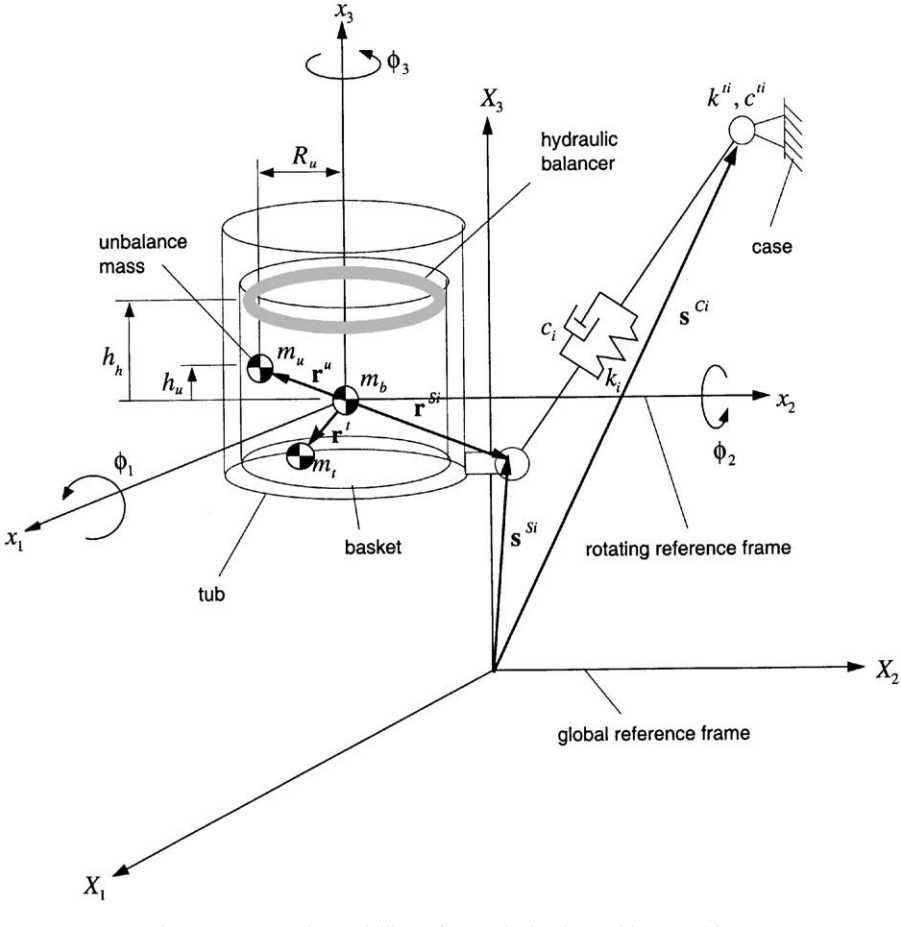

Figure 7. Dynamic modelling of a vertical axis washing machine.

When small motions are assumed, the translational displacements of the tub and the unbalance mass can be written as

$$\mathbf{x}^t = \mathbf{x}^b + \mathbf{Q}\mathbf{r}^t, \tag{13}$$

$$\mathbf{x}^u = \mathbf{x}^b + \mathbf{Q}\mathbf{r}^u, \tag{14}$$

where

$$\mathbf{Q} = \begin{bmatrix} 1 & \phi_3 & -\phi_2 \\ -\phi_3 & 1 & \phi_1 \\ \phi_2 & -\phi_1 & 1 \end{bmatrix} \tag{15}$$

and $\mathbf{r}^t = [r_1^t \; r_2^t \; r_3^t]^{\mathrm{T}}$, $\mathbf{r}^u = [R_u \cos\theta \; R_u \sin\theta \; h_u]^{\mathrm{T}}$. R_u and h_u represent the rotational radius and height of the unbalance mass, respectively, as shown in Figure 7. Note that $\mathbf{Q}$ represents the rotational transformation matrix that relates the rotating frame to the global reference frame. The rotational velocities of the basket and the tub are written as

$$\dot{\boldsymbol{\psi}}^b = \mathbf{Q}\dot{\boldsymbol{\phi}} + \boldsymbol{\omega}, \tag{16}$$

$$\dot{\boldsymbol{\psi}}^t = \mathbf{Q}\dot{\boldsymbol{\phi}}, \tag{17}$$

where $\boldsymbol{\omega} = [0 \; 0 \; \dot{\theta}]^{\mathrm{T}}$ is the angular velocity vector of the basket with respect to the tub, and θ is the spin angle.

The kinetic energy of the system is given by

$$T = \tfrac{1}{2} m_b \| \dot{\mathbf{x}}^b \|^2 + \tfrac{1}{2} m_t \| \dot{\mathbf{x}}^t \|^2 + \tfrac{1}{2} m_u \| \dot{\mathbf{x}}^u \|^2 + \tfrac{1}{2} (\dot{\boldsymbol{\psi}}^b)^{\mathrm{T}} \mathbf{I}_b \dot{\boldsymbol{\psi}}^b + \tfrac{1}{2} (\dot{\boldsymbol{\psi}}^t)^{\mathrm{T}} \mathbf{I}_t \dot{\boldsymbol{\psi}}^t, \tag{18}$$

where m_b, m_t, and m_u represent the masses of the basket, tub, and unbalance, respectively, and $\mathbf{I}_b$ and $\mathbf{I}_t$ are the inertia tensors of the basket and tub respectively. The rotational kinetic energy of the unbalance mass is included in the inertia tensor of basket by treating it as a point mass, because the unbalance mass is rotating together with the basket. Since the force exerted by the hydraulic balancer will be included, the kinetic energy of the hydraulic balancer is not necessary in equation (18). The gravitational potential energy of the system is given by

$$V_g = (m_b x_3^b + m_t x_3^t + m_u x_3^u) g. \tag{19}$$

Forces due to the spring and damper of the suspension rod can be written as

$$F_{SDx_j} = -\sum_{i=1}^{4} (k_i \delta_i + c_i v_i) \frac{\partial L_i}{\partial x_j^b} \quad (j = 1, 2, 3), \tag{20}$$

$$F_{SD\phi_j} = -\sum_{i=1}^{4} (k_i \delta_i + c_i v_i) \frac{\partial L_i}{\partial \phi_j} \quad (j = 1, 2, 3), \tag{21}$$

respectively, where $L_i = \| \mathbf{x}^{Si} - \mathbf{x}^{Ci} \|$, $\delta_i = L_i - L_{0i}$, and $v_i = \dot{\mathbf{x}}^{Si} \cdot \mathbf{e}^i$. Here, k_i and c_i are the spring stiffness and damping coefficient, L_{0i} and L_i are the initial and deformed lengths of the suspension rod, and $\mathbf{e}^i$ is the unit vector in the direction of the suspension rod.

Next, the forces due to the hydraulic balancer can be derived from the displacement of the centroid of the hydraulic balancer. Figure 8 shows the relation between the centroid of the hydraulic balancer, c, and the eccentricity of the center of the hydraulic balancer tube, e. In section 2, it was already shown that the relation could be expressed as that in the form of equation (6) when small motions were assumed. For the steady state rotation, the centroid of the hydraulic balancer will rotate with constant radius $(e + c)$ about the X_3-axis of the

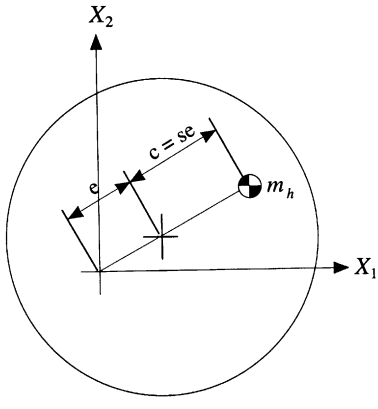

Figure 8. Motion of the hydraulic balancer.

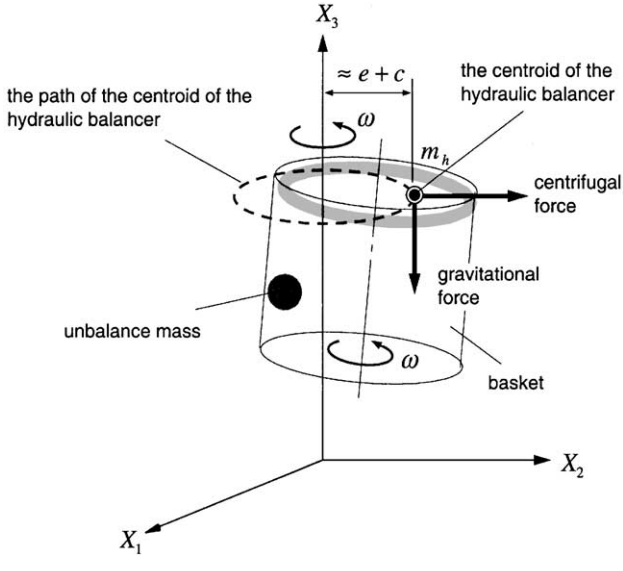

Figure 9. The forces due to the hydraulic balancer.

global reference frame. The forces due to the hydraulic balancer are thus the centrifugal and gravitational forces, as shown in Figure 9. The displacement of the centroid of the hydraulic balancer, $\mathbf{s}^h$, may then be calculated from the displacement of the center of the balancer tube. The planar components of $\mathbf{s}^h$ are the products of $(1 + c/e)$ and the planar components of the position vector of the center of the balancer tube. The vertical component of $\mathbf{s}^h$ is assumed to be the same as the vertical component of the position vector of the center of balancer tube. Thus, the position vector of the centroid of the hydraulic balancer can be written as

$$\mathbf{s}^h = \begin{Bmatrix} s_1^h \\ s_2^h \\ s_3^h \end{Bmatrix} = \begin{Bmatrix} (1 + c/e)(s_{01}^b + x_1^b + h_h\phi_2) \\ (1 + c/e)(s_{02}^b + x_2^b - h_h\phi_1) \\ s_{03}^b + x_3^b + h_h \end{Bmatrix}, \tag{22}$$

where $\mathbf{s}_0^b$ is the initial position vector of the basket and h_h is the vertical distance of the hydraulic balancer from the mass center of the basket. The acceleration of the hydraulic balancer can then be obtained by differentiating equation (22) twice:

$$\ddot{\mathbf{x}}^h = \frac{\partial^2}{\partial t^2}\mathbf{s}^h = \begin{Bmatrix} (1 + c/e)(\ddot{x}_1^b + h_h\ddot{\phi}_2) \\ (1 + c/e)(\ddot{x}_2^b - h_h\ddot{\phi}_1) \\ \ddot{x}_3^b \end{Bmatrix}. \tag{23}$$

Consequently, the balancing force and moment due to the hydraulic balancer can be written in terms of the inertia and gravitational forces and their moment around the mass center of the basket:

$$\mathbf{F}_{HB} = m_h \begin{Bmatrix} -\ddot{x}_1^h \\ -\ddot{x}_2^h \\ -\ddot{x}_3^h + g \end{Bmatrix} \equiv \begin{Bmatrix} F_{HBx_1} \\ F_{HBx_2} \\ F_{HBx_3} \end{Bmatrix}, \tag{24}$$

$$\mathbf{M}_{HB} = (\mathbf{s}^h - \mathbf{s}_0^b - \mathbf{x}^b) \times \mathbf{F}_{HB} \equiv \begin{Bmatrix} F_{HB\phi_1} \\ F_{HB\phi_2} \\ F_{HB\phi_3} \end{Bmatrix}. \tag{25}$$

From the kinetic and potential energies and spring and damping forces that were derived above, dynamic equations of motion of the washing machine system can be derived by Lagrange's equation, such as

$$\frac{\mathrm{d}}{\mathrm{d}t}\left(\frac{\partial T}{\partial \dot{x}_j^b}\right) - \frac{\partial T}{\partial x_j^b} + \frac{\partial V_g}{\partial x_j^b} = F_{SDx_j} + F_{HBx_j} \quad (j = 1, 2, 3), \tag{26}$$

$$\frac{\mathrm{d}}{\mathrm{d}t}\left(\frac{\partial T}{\partial \dot{\phi}_j}\right) - \frac{\partial T}{\partial \phi_j} + \frac{\partial V_g}{\partial \phi_j} = F_{SD\phi_j} + F_{HB\phi_j} \quad (j = 1, 2, 3). \tag{27}$$

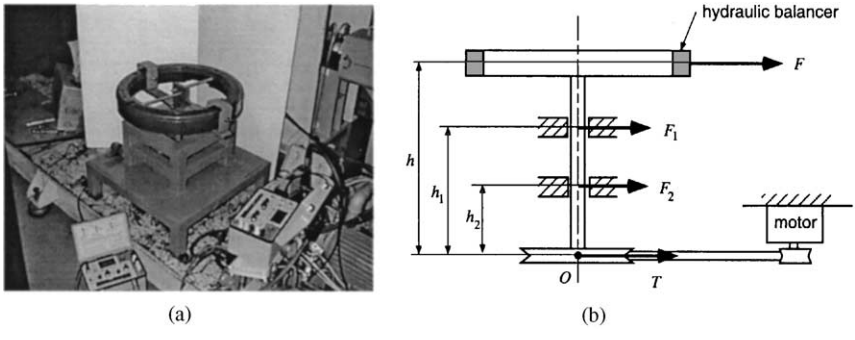

Figure 10. Test apparatus to measure the centrifugal force of the hydraulic balancer: (a) the experimental set-up, and (b) free body diagram.

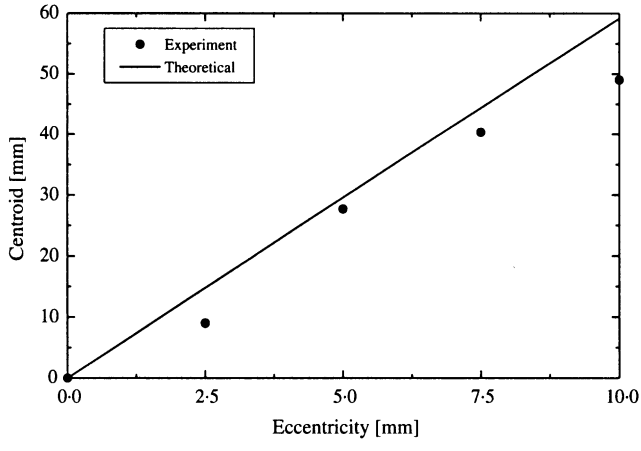

Figure 11. Centroid change due to the eccentricity change.

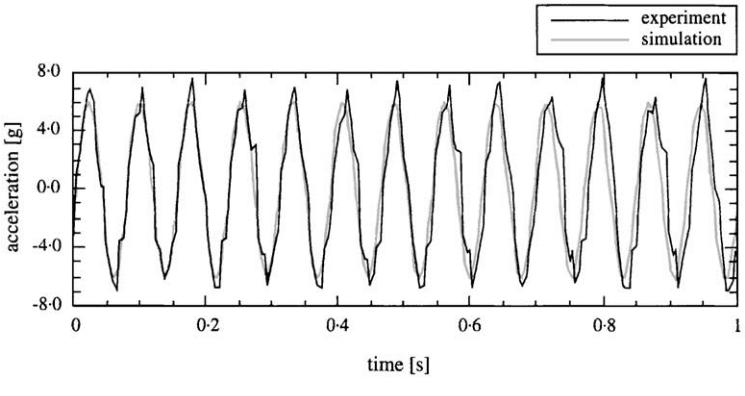

Figure 12. The radial acceleration at the top of the tub.

The resulting dynamic equations of motion can be written in the matrix form as

$$\mathbf{A}\ddot{\mathbf{x}} = \mathbf{b}, \tag{28}$$

where $\mathbf{x} = [x_1^b\ x_2^b\ x_3^b\ \phi_1\ \phi_2\ \phi_3]^{\mathrm{T}}$ is a state vector, and $\mathbf{A}$ and $\mathbf{b}$ are 6×6 and 6×1 system matrices respectively. The components of the matrices are summarized in Appendix A. A Runge–Kutta fourth order integration algorithm was used to solve these equations.

3. VALIDATION WITH EXPERIMENTS

The test apparatus to measure centrifugal force of the hydraulic balancer is shown in Figure 10(a). During the steady state rotation of the hydraulic balancer rotated by the washing machine motor, strains acting on the bars supporting the rotating axis, which is converted to force quantities, have been measured while increasing the eccentricity by 2·5 mm up to 10 mm. Eccentricity is limited to 10 mm in the range of linear relation satisfying equation (6) because of excessive force. By considering free body diagram of Figure 10(b), centrifugal force F is obtained as

$$F = -\frac{F_1 h_1 + F_2 h_2}{h}. \tag{29}$$

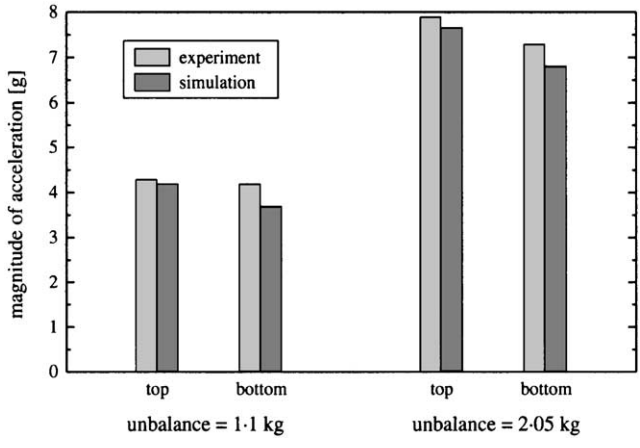

Figure 13. Comparison of the experiment and the simulation.

TABLE 1

Parameters for analysis

Parameters	Unit	Nominal value	Lower limit	Upper limit
Suspension spring stiffness	N/m	2871	1000	4000
Suspension length	m	0·595	0·55	0·65
Mass of the basket	kg	6·755	4·0	10·0
Mass of the tub	kg	15·31	10·0	25·0
C.g. height of the basket	m	0·520	0·47	0·57
C.g. height of the tub	m	0·315	0·25	0·36
Mass of the hydraulic balancer	kg	2·565	1·5	4·0
Volumetric ratio of the hydraulic balancer	—	0·5	0·3	0·7
Inner radius of the hydraulic balancer	m	0·206	0·17	0·23

The centroid of the fluid can be calculated from centrifugal force by equation (3). Figure 11 shows centroid change due to eccentricity by comparing theoretical analysis and experimental result. Centroid change in experiment is less than that of theoretical analysis. The reason is presumed to be the fact that the orifice of the tube to obstruct transient effect of hydraulic balancer has some influence on steady state as well. However, since the results have shown good agreement, this indicates that it is possible to predict the effect of hydraulic balancer from theoretical analysis presented here.

For the validation of the mathematical model, the experiments of spin drying procedure were performed. The unbalance masses of 1·1 and 2·05 kg were attached to the basket, and accelerometers were attached to the top and the bottom of the tub to measure the radial accelerations. Although the tub is actually asymmetric in the horizontal plane because of the driving unit such as motor and transmission, in the simulation it is assumed symmetric.

Figure 12 shows the experimental and the simulation results of the radial acceleration at the top of the tub when the unbalance mass of 1·1 kg was attached. To compare the results of the experiment and the simulation, the mean magnitude of the radial acceleration of the experiment was calculated by fitting process. Figure 13 shows the comparison of the results of the experiment and the simulation. The compared values are the magnitudes of the radial

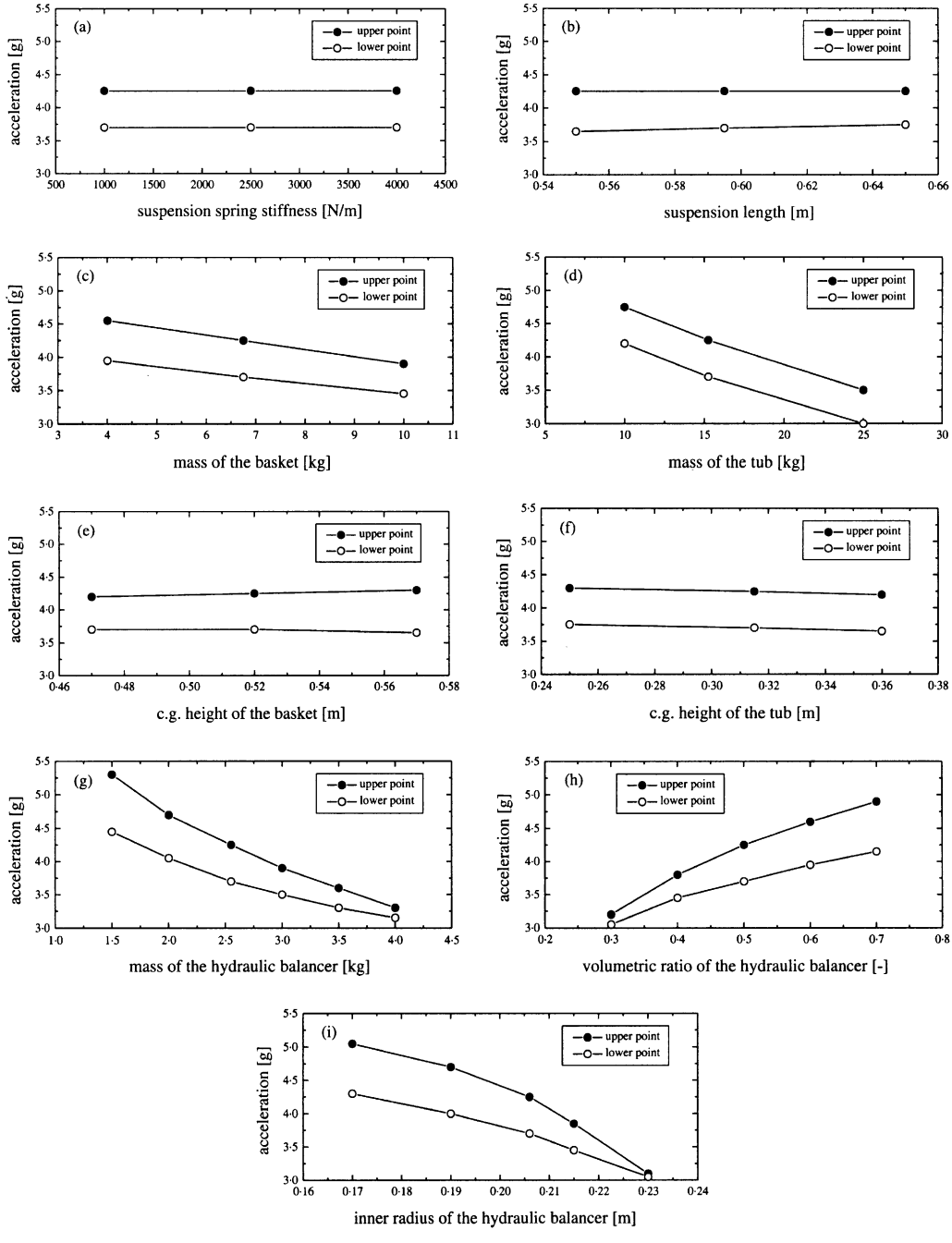

Figure 14. The effect of the change of the parameters.

acceleration at the top and the bottom of the tub. The results of the simulation show good agreement with those of experiment. The main reasons for the differences between the simulation and the experiment are the errors in measuring or assuming the parameters, the assumption in modelling the hydraulic balancer, and the ignorance of asymmetry of the tub.

4. PARAMETER STUDY

We considered only those parameters whose values are actually variable, and the range of the variation is limited to the actual bounds. Table 1 shows the parameters for analysis, their nominal values, upper limits, and lower limits. Due to the differences in the unit of the parameters, we used the simple method wherein the parameters are changed in two or more levels from the nominal values instead of using the sensitivity analysis. The analysis is performed using an unbalance mass of 1·1 kg, and the magnitudes of the steady state radial acceleration are investigated as the index of the analysis.

The results of the parameter analysis are shown in Figure 14. From Figure 14(a, b), we can see that the suspension spring stiffness and the length of the suspension have little influence on the vibration of the washing machine. These parameters are related with the suspension. There is another parameter related to the suspension: the damping coefficient. However, this is excluded, because the damper is filled with air and not with fluid. Therefore, it is difficult to modify. Figure 14(c, d) shows the influence of the masses of the basket and the tub. We can see that the increases of the masses of the basket and the tub greatly reduce the accelerations. Increase in mass of 3 kg has a great effect on the reduction of vibration. In case of the tub, increase in mass of 10 kg has a great effect on the reduction of vibration. The reason is that the large mass of the basket reduces the eccentricity of the total system with the unbalance mass. Therefore, increase in masses of the basket and the tub has a great influence on the reduction of vibration. However, there are actually many limits in increasing the mass. Figure 14(e, f) shows the influence of the c.g. height of the basket and the tub. We can see that these values have little influence. There are three parameters related with the hydraulic balancer: the mass of the hydraulic balancer, the volumetric ratio of the hydraulic balancer, and the inner radius of the hydraulic balancer tube. The outer radius of the hydraulic balancer tube was excluded, since the value of the outer radius is difficult to modify because of the packaging problem. Figure 14(g) illustrates the effect of the change in the mass of the hydraulic balancer with constant volume ratio of the fluid to the tube. We can see that the increase in the mass of the hydraulic balancer reduces the vibration, and this is more evident at the upper point than at the lower point. Moreover, the greater the mass of the hydraulic balancer, the lower the reduction in the amount of the vibration. Figure 14(h) shows the effect of the change in the volumetric ratio with constant mass of the hydraulic balancer. It shows that the small volume ratio reduces the vibration. The reason is that the small volumetric ratio increases the eccentricity of the fluid during spin drying. Figure 14(i) shows the effect of the change in the inner radius of the hydraulic balancer with constant volume and outer radius of the hydraulic balancer. It shows that the large inner radius reduces the vibration due to the increase of the centroid of the fluid. Due to the above reason, the cross section of the hydraulic balancer should be skinny and tall.

From these studies, it can be seen that the vibration will be reduced by increasing the mass, decreasing the volumetric ratio, and increasing the inner radius of the hydraulic balancer. Therefore, we can predict that the proper design of the hydraulic balancer will greatly improve the performance of the washing machine.

5. CONCLUSION

In this paper, the analytical formulations of a hydraulic balancer as well as a vertical axis washing machine are presented. From a whirling model of a washing machine, the centrifugal force of the hydraulic balancer can be calculated from the eccentricity of the

unbalance mass and the centroidal distance of the fluid balancer. In addition, the centroidal distance shows the linear relation with the eccentricity when the eccentricity is small, and in the limited case, the centroidal distance approaches a certain value. From the experiment of the hydraulic balancer, the linear relation between the eccentricity and the centroidal distance was validated.

Comparing the simulation with the experiment, the mathematical model presented in this paper shows good agreement with the actual behavior of the washing machine. To investigate which parameters have an effect on the vibration of the washing machine, a parameter study was performed. From the parameter study, it was observed that the vibration would be reduced by increasing the mass, decreasing the volumetric ratio, and increasing the inner radius of the hydraulic balancer. Therefore, the effect of the hydraulic balancer may be maximized when the density of the fluid in the hydraulic balancer should be large. This is the reason why the salt water is more effective working fluid than the fresh water or the oil. To improve the performance of the washing machine, proper design of the hydraulic balancer was presented in this paper.

ACKNOWLEDGMENTS

This work was supported by the Brain Korea 21 Project, Mechanical Engineering Research Division and Daewoo Electronics Co., Ltd.

REFERENCES

1. B. S. BAGEPALLI 1987 *ASME* 11*th Biannual Conference of Mechanical Vibrations and Noise*, 13–18. Dynamic modeling of washing machine suspension systems.
2. O. S. TURKEY, I. T. SUMER and A. K. TUGCU 1992 *Advances in Design Automation Conference*, *ASME Proceedings* **DE44-1**, 383–390. Modeling and dynamic analysis on the suspension system of a front loaded washing machine.
3. I. T. SUMER, A. K. TUGCU and O. S. TURKAY 1992 *Proceedings of* 43*rd Annual International Appliances Technical Conference*, 117–127. The use of suspension system modeling and simulation in the manufacturing of washing machines.
4. O. S. TURKAY, A. K. TUGCU, I. T. SUMER and B. KIRAY 1993 *Advances in Design Automation Conference*, *ASME Proceedings* **DE65-1**, 125–132. Suspension design optimization of a washing machine: Part I. Modeling and validation results.
5. O. S. TURKAY, A. K. TUGCU, I. T. SUMER and B. KIRAY 1993 *Advances in Design Automation Conference*, *ASME Proceedings* **DE65-1**, 133–144. Suspension design optimization of a washing machine: Part II. Formulation and implementation of parametric optimization.
6. D. C. CONRAD and W. SOEDEL 1995 *Journal of Sound and Vibration* **188**, 301–314. On the problem of oscillatory walk of automatic washing machines.
7. L. MEIROVITCH 1986 *Elements of Vibration Analysis*. New York: McGraw-Hill.

APPENDIX A: SYSTEM MATRICES

The matrix **A** in equation (28) is a symmetric matrix and the components are given as

$$a_{11} = a_{22} = m_b + m_t + m_u + m_h\left(1 + \frac{c}{e}\right)$$

$$a_{33} = m_b + m_t + m_u + m_h$$

$$a_{12} = a_{13} = a_{14} = 0$$

$$a_{15} = m_t r_3^t + m_u h_u + m_h h_h\left(1 + \frac{c}{e}\right)$$

$$a_{16} = -m_t r_2^t - m_u R_u \sin\theta$$

$$
\begin{aligned}
a_{23} &= a_{25} = 0\\
a_{24} &= -a_{15}\\
a_{26} &= m_t r_1^t + m_u R_u \cos\theta\\
a_{34} &= -a_{16}\\
a_{35} &= -a_{26}\\
a_{36} &= 0\\
a_{44} &= m_t\{(r_2^t)^2 + (r_3^t)^2\} + m_u(R_u^2\sin^2\theta + h_u^2) + m_h h_h^2\left(1+\frac{c}{e}\right)\\
&\quad + I_{t11} + 2(I_{t12}\phi_3 - I_{t31}\phi_2),\\
a_{45} &= -m_t r_1^t r_2^t - m_u R_u^2\cos\theta\sin\theta - I_{t12} + I_{t31}\phi_1 - I_{t23}\phi_2\\
&\quad + (I_{t11} - I_{t22})\phi_3,\\
a_{46} &= -m_t r_3^t r_1^t - m_u R_u h_u\cos\theta - I_{t31} - I_{t12}\phi_1 + (I_{t33} - I_{t11})\phi_2\\
&\quad + I_{t23}\phi_3,\\
a_{55} &= m_t\{(r_3^t)^2 + (r_1^t)^2\} + m_u(R_u^2\cos^2\theta + h_u^2) + m_h h_h^2\left(1+\frac{c}{e}\right)\\
&\quad + I_{t22} + 2(I_{t23}\phi_1 - I_{t12}\phi_3),\\
a_{56} &= -m_t r_2^t r_3^t - m_u R_u h_u\sin\theta - I_{t23} + (I_{t22} - I_{t33})\phi_1 + I_{t12}\phi_2\\
&\quad - I_{t31}\phi_3,\\
a_{66} &= m_t\{(r_1^t)^2 + (r_2^t)^2\} + m_u R_u^2 + I_{t33} + 2(I_{t31}\phi_2 - I_{t23}\phi_1).
\end{aligned}
$$

The components of **b** in equation (28) are given as

$$
\begin{aligned}
b_1 &= F_{SDx1} + m_u R_u\{(\dot\theta^2 + 2\dot\phi_3\dot\theta + \phi_3\ddot\theta)\cos\theta + (-\phi_3\dot\theta^2 + \ddot\theta)\sin\theta\},\\
b_2 &= F_{SDx2} + m_u R_u\{(\phi_3\dot\theta^2 - \ddot\theta)\cos\theta + (\dot\theta^2 + 2\dot\phi_3\dot\theta + \dot\phi_3\ddot\theta)\sin\theta\}\\
b_3 &= F_{SDx3} - (m_b + m_t + m_u + m_h)g\\
&\quad + m_u R_u\{(\phi_2\dot\theta^2 + 2\dot\phi_1\dot\theta + \phi_1\ddot\theta)\cos\theta + (-\phi_1\dot\theta^2 + 2\dot\phi_2\dot\theta + \phi_2\ddot\theta)\sin\theta\},\\
b_4 &= F_{SD\phi1} - \left[m_t r_2^t + m_u R_u\sin\theta + m_h\left\{\frac{c}{e}x_2 - \left(1+\frac{c}{e}\right)h_h\phi_1\right\}\right]g\\
&\quad + m_u R_u h_u\{(-\phi_3\dot\theta^2 + \ddot\theta)\cos\theta - (\dot\theta^2 + 2\dot\phi_3\dot\theta + \phi_3\ddot\theta)\sin\theta\}\\
&\quad - m_u R_u^2\sin\theta\{(\phi_2\dot\theta^2 + 2\dot\phi_1\dot\theta + \phi_1\ddot\theta)\cos\theta + (-\phi_1\dot\theta^2 + 2\dot\phi_2\dot\theta + \phi_2\ddot\theta)\sin\theta\}\\
&\quad + 2\{\dot\phi_1(I_{t31}\dot\phi_2 - I_{t12}\dot\phi_3) + \dot\phi_2(I_{t22}\dot\phi_3 + I_{t23}\dot\phi_2) - \dot\phi_3(I_{t33}\dot\phi_2 + I_{t23}\dot\phi_3) - I_{b33}\dot\phi_2\dot\theta\},\\
b_5 &= F_{SD\phi2} + \left[m_t r_1^t + m_u R_u\cos\theta + m_h\left\{\frac{c}{e}x_1 + \left(1+\frac{c}{e}\right)h_h\phi_2\right\}\right]g\\
&\quad + m_u R_u h_u\{(\dot\theta^2 + 2\dot\phi_3\dot\theta + \phi_3\ddot\theta)\cos\theta - (\phi_3\dot\theta^2 - \ddot\theta)\sin\theta\}\\
&\quad + m_u R_u^2\cos\theta\{(\phi_2\dot\theta^2 + 2\dot\phi_1\dot\theta + \phi_1\ddot\theta)\cos\theta + (-\phi_1\dot\theta^2 + 2\dot\phi_2\dot\theta + \phi_2\ddot\theta)\sin\theta\}\\
&\quad + 2\{-\dot\phi_1(I_{t11}\dot\phi_3 + I_{t31}\dot\phi_1) + \dot\phi_2(I_{t12}\dot\phi_3 - I_{t23}\dot\phi_1) + \dot\phi_3(I_{t33}\dot\phi_1 + I_{t31}\dot\phi_3) + I_{b33}\dot\phi_1\dot\theta\},\\
b_6 &= F_{SD\phi3} + m_u R_u^2(\phi_3\dot\theta^2 - \ddot\theta) - I_{b33}\ddot\theta\\
&\quad + 2\{\dot\phi_1(I_{t11}\dot\phi_2 + I_{t12}\dot\phi_1) - \dot\phi_2(I_{t22}\dot\phi_1 + I_{t12}\dot\phi_2) + \dot\phi_3(I_{t23}\dot\phi_1 - I_{t31}\dot\phi_2)\}.
\end{aligned}
$$